Supporting Information

Kriegel et al. 10.1073/pnas.0908957106

SI Materials and Methods

Generation of *Grail*-Deficient Mice. A 129SV/J genomic library was screened with murine *Grail* cDNA to obtain genomic clones encompassing *Grail*. The Cre-loxP system was used as a targeting strategy to delete exons 4, 5, and 6 coding for the highly conserved RING finger domain (see Fig. 1*A*). The target region of *Grail* was cloned into the targeting vector pEASY-flox (kindly provided from K. Rajewsky, Harvard Medical School, Boston). The targeting vector was linearized and electroporated into ES cells (TC1). Targeted clones were identified by Southern blot analysis as shown in Fig. 1*B* and treated with Cre enzyme in vitro to delete *Grail* exons 4 to 6 flanked by loxP sites, causing an out-of-frame mutation. Two deleted ES subclones were identified by RT-PCR analysis. Each subclone was injected into C57BL/6 blastocysts and transferred into pseudopregnant foster mothers. The resulting male chimeric mice were bred to C57BL/6 females to obtain +/− mice. *Grail*$^{-/-}$ were obtained by additional crossing with heterozygous mice (N.B.: *Grail*$^{-/-}$ is used for simplicity throughout the main text although male *GRAIL*$^{Y/-}$ were used in some experiments that are comparable to female KO mice). Successful deletion of *Grail* was verified by real-time and RT-PCR analyses (Fig. 1*C*, Fig. S1). Loss of protein expression was confirmed by Western blot analysis from various solid organ tissues (Fig. 1*D*). Mice were backcrossed at least eight times for experimental analysis. Genotyping of wild-type and knockout mice was performed with the following primers for *Grail*: WT forward primer, 5′-CCAAAATCGATTCTCGTGGCTCC-3′; WT reverse primer, 5′-GGGCAAGTCCTGTGTTCTAAAAGC-3′; KO forward primer, 5′-GCTGAAGTTAGTACTGCATG-3′; KO reverse primer, 5′-GTCAACAGGTGGCAGATACC-3′.

Mice. C57BL/6J mice were obtained from The Jackson Laboratory. Foxp3-IRES-mRFP (FIR) mice were described in ref. 19. In these C57BL/6 mice, a bicistronic fluorescent reporter was knocked into the endogenous *Foxp3* locus, allowing identification of Foxp3 expression. When Foxp3 gene expression is turned on, a monomeric red fluorescent protein (mRFP) is coexpressed which can be detected by flow cytometry. It has been demonstrated that this knockin does not to interfere with FOXP3$^+$ Treg function (19). FIR mice were crossed with *Grail*$^{-/-}$ mice for Treg experiments as described below. Wildtype, transgenic and KO mice were maintained in specific pathogen-free barrier facilities at Yale University. All animal experiments were approved by the Institutional Animal Care and Use Committee of Yale University.

Cell Culture. In vitro cultures were performed using purified T cells in Bruffs medium supplemented with 10% FCS, 2 mM L-Glutamine, 1% Penicillin-Streptomycin and 1 mM nonessential amino acids. To assess viability, cells were harvested, stained with 1 μg/mL of propidium iodide (Sigma–Aldrich) and analyzed by flow cytometry.

Flow Cytometry and Cell Sorting. Single cell suspensions were analyzed by flow cytometry using FACS SCAN, FACS Calibur or LSRII and CELLQuest software, FACS Diva software (BD Biosciences) or FlowJo software (Tree Star, Inc., Ashland, OR), respectively. Cell sorting of defined subpopulations was performed using FACSAria cell sorter (BD Biosciences, San Jose, CA). The following monoclonal antibodies (all from BD PharMingen except where noted otherwise) were used: CD3, CD4, CD8, CD11b, CD19, CD25, CD40L, CD44, CD62L, CD127 (eBioscience), B220 and NK1.1. Cells stained with biotinylated monoclonal antibodies were incubated with fluorochrome-conjugated streptavidin-PE, streptavidin-PerCP, streptavidin-APC and streptavidin-APC-Cyc7 (BD PharMingen). All fluorescence intensity plots are shown in log scales.

T cell sorting was performed either by MACS using CD4 conjugated microbeads or by flow cytometry. T cell subsets such as naïve (CD4$^+$ CD25$^-$ CD44$^-$ CD62L$^+$), effector (CD4$^+$ CD25$^-$ CD44$^+$ CD62L$^+$) and memory (CD4$^+$ CD25$^-$ CD44$^+$ CD62L$^-$) were isolated based on the indicated phenotype. FOXP3$^+$ cells from FIR mice were sorted based on red fluorescence as described in ref. 19.

In Vitro Anergy Induction. For ionomycin-induced anergy studies, sorted naïve (CD25$^-$ CD44$^-$ CD62L$^+$) CD4$^+$ T cells were initially stimulated with plate bound anti(α)-CD3ε (1 μg/mL) and soluble α-CD28 (5 μg/mL) for 2 days. Cells were rested for 3 additional days. Cells were harvested and live cells were separated by density gradient centrifugation. Cells were plated and cultured either in the presence or in the absence of ionomycin at indicated concentrations for 12 h. Cells were harvested, washed and restimulated in the presence of plate bound α-CD3ε (5 μg/mL) and soluble α-CD28 (2 mg/mL) for 24–48 h. Proliferation was measured after 48 h by ^{3}H-thymidine incorporation.

For TGF-β-induced anergy studies, sorted naïve (CD25$^-$ CD44$^-$ CD62L$^+$) CD4$^+$ T cells were initially stimulated with plate bound α-CD3ε (5 μg/mL) and soluble α-CD28 (2 mg/mL) for 5 days either in the presence or in the absence of TGF-β (2 ng/mL). Cells were harvested, washed and restimulated in the presence of plate bound α-CD3ε (5 μg/mL) and soluble α-CD28 (2 μg/mL) for 48 h.

For CD4$^+$CD25$^+$ regulatory T cell-mediated anergy induction, sorted naïve (CD25$^-$ CD44$^-$ CD62L$^+$) CD4$^+$ T cells were labeled with CFSE and incubated with equal ratio of CD4$^+$ CD25$^+$ CD44$^-$ CD62L$^+$ T cells along with 5-μm latex beads (Interfacial Dynamics) coated with α-CD3ε (2.5 μg/mL) and α-CD28 (1.25 μg/mL) for 24 h. Cells were harvested and CFSE$^+$ T cells were resorted by FACS. Sorted cells were restimulated in the presence of antibody coated latex beads for 48 h.

In Vitro FOXP3$^+$ Treg Suppressor Cell Assay. Sorted naïve CD4$^+$ T cells were cocultured with equal ratio of CD4$^+$CD25$^+$ mRFP$^+$ Tregs obtained from Foxp3-IRES-mRFP (FIR) *Grail*$^{+/+}$ and *Grail*$^{-/-}$ mice. As described above, mRFP$^+$ cell isolation from FIR mice selects specifically for FOXP3 expressing cells (19). Naïve and FOXP3$^+$ cells were stimulated with 5-μm latex beads (Interfacial Dynamics) coated with α-CD3ε (2.5 μg/mL) and α-CD28 (1.25 μg/mL) for 48 h. Cell proliferation was measured by ^{3}H-thymidine incorporation during the last 12 h of culture. IL-2 levels were measured by ELISA.

Oral Tolerance to Ovalbumin. Ovalbumin (20 mg/mL) was administered to *Grail*$^{+/+}$ OT-II or *Grail*$^{-/-}$ OT-II TCR transgenic mice in their drinking water for 5 days. PBS fed OT-II TCR transgenic mice served as controls. On day 6, spleen and lymph node CD4$^+$ T cells were sorted and stimulated in vitro in the presence of irradiated APCs pulsed with various concentrations of OVA323–339 peptide. Proliferation was measured after 48 h by ^{3}H-thymidine incorporation, IL-2 levels in the supernatants by ELISA, and cell cycling based on CFSE dilution after 72 h by flow cytometry.

Oral Tolerance Induction in Experimental Allergic Encephalitis (EAE). *Grail*$^{+/+}$ or *Grail*$^{-/-}$ mice were initially fed with 25 mg of mouse myelin basic protein (MBP) dissolved in 0.5 mL of PBS by gastric intubation on alternating days over a 10 day period with an 18 gauge stainless steel feeding needle.

For EAE studies, each mouse received a s.c. injection in the flank with 400 μg of mouse MBP in 0.15 mL of PBS emulsified in an equal volume of complete Freund's adjuvant (CFA) containing 4 mg of *Mycobacterium tuberculosis* H37 RA per mL. Pertussis toxin (200 ng per mouse per injection) was given intravenously at the time of immunization and 48 h later. Animals were scored for EAE as follows: 0, no disease; 1, tail paralysis; 2, hind limb weakness; 3, hind limb paralysis; 4, hind limb plus forelimb paralysis; 5, moribund.

T Cell Proliferation and IL-2 Secretion. Naïve (CD25$^-$ CD44$^-$ CD62L$^+$) CD4$^+$ T cells were sorted and labeled with CFSE (3 μM) at 37 °C for 10 min. Cells were stimulated with indicated concentrations of plate bound αCD3ε and soluble αCD28. At indicated time points, cells were harvested and analyzed by flow cytometry.

For experiments involving secondary stimulation, primary stimulated T cells were harvested, washed and live cells were separated through gradient centrifugation. Cells were restimulated with plate bound α-CD3ε (5 μg/mL) and soluble α-CD28 (2 μg/mL). At indicated time points, cell proliferation was measured by either ^{3}H-thymidine incorporation and/or analyzed by flow cytometry (CFSE labeled cells).

For IL-2 detection experiments, sorted naïve CD4$^+$ T cells from *Grail*$^{+/+}$ and *Grail*$^{-/-}$ mice were stimulated with plate-bound α-CD3ε (5 μg/mL) and soluble α-CD28 (2 μg/mL). 48 h after stimulation, supernatants were collected and IL-2 cytokine levels were determined by ELISA.

In Vitro T Cell Differentiation. Naïve (CD25$^-$ CD44$^-$ CD62L$^+$) CD4$^+$ T cells were sorted and stimulated with plate bound α-CD3ε (5 μg/mL) and soluble α-CD28 (2 μg/mL) for 5 days under conditions that promote Th0 [in the presence of IL-2 (50 units/mL), α-IL-4 (5 μg/mL) and α-IFN-γ (5 μg/mL)], Th1 [in the presence of IL-2 (50 units/mL), α-IL-4 (5 μg/mL) and IL-12 (3.5 ng/mL)], Th2 [in the presence of IL-2 (50 units/mL), IL-4 (500 units/mL) and α-IFN-γ (5 μg/mL)] and Th17 [in the presence of α-IFN-γ (10 μg/mL), α-IL-4 (10 μg/mL), α-IL-2 (10 μg/mL) TGF-β (2 ng/mL), IL-6 (20 ng/mL) and IL-23 (20 ng/mL)]. Medium and cytokine cocktails were replenished at day 2 of each differentiation culture.

Calcium Flux. Sorted CD4$^+$ T cells were labeled with Fluo3-AM (molecular probes) for 30 min at 37 °C. Cells were washed and labeled with α-CD3ε biotin. Cells were washed, prewarmed with medium and calcium release was measured after cross linking with streptavidin. In some experiments, sorted CD4$^+$ T cells were prewarmed and calcium release was measured after addition of ionomycin (100 ng/mL).

RNA Extraction and Real-Time PCR. Total RNA was isolated using commercially available kit systems ("Absolutely RNA mini prep kit"—Stratagene). cDNA was synthesized using oligo dT primer and SuperScript II RT (Invitrogen). The PCR was performed in duplicates or triplicates using 7500 real time PCR systems and power SYBR Green PCR master mix (Applied Biosystems) or TaqMan probe (Applied Biosystems), respectively, according to the manufacturer's instructions. The following primer and probe sequences for *Grail* were used for TaqMan real-time PCR: forward primer, 5′-GCTGCGCACCTTGAAACAA-3′; reverse primer, 5′-AGCTCAATGCACACAGCACAG-3′; probe, 5′-AGACAAGGAAATTGGCCCTGATGGAGAT-3′

Western Blot Analysis, Immunoprecipitation, and ELISA. For Western blot analysis, 20 μg of protein was loaded on 3–8% TA gel (Invitrogen), separated by electrophoresis and blotted onto nylon membranes. The membranes were treated with primary antibodies specific for GRAIL (BD Pharmigen), *p*-Zap70, Zap70, *p*-PLCγ1, PLCγ1, Calcineurin A, NFATc4, *p*-MEK1/2, MEK1/2, *p*-p38, p38, *p*-JNK, JNK, PKCθ, pERK1/2, ERK1/2, *p*-NF-κB, NF-κB (all from Cell Signaling) and Actin (Santa Cruz Biotechnology) followed by staining with secondary antibodies conjugated to horse radish peroxidase. The enzymatic reaction was visualized using SuperSignal West Pico Chemiluminescent Substrate Kit (Pierce).

Western blots were performed with lysates from sorted splenic CD4$^+$ T cells that were either unstimulated or activated with α-CD3 (5 μg/mL) and α-CD28 (2 μg/mL) for 30 min.

For interaction studies, sorted splenic CD4$^+$ T cells of *Grail*$^{+/+}$ and *Grail*$^{-/-}$ mice were stimulated with plate bound α-CD3ε (5 μg/mL) and soluble α-CD28 (2 μg/mL) for 1 h. Immunoprecipitation was performed with GRAIL antibodies using a commercially available kit (Upstate) according to manufacturer's instructions.

ELISAs for IL-2, IL-4, IL-17 and IFN-γ were performed using commercially available ELISA kits according to the manufacturer's instructions (BD Pharmigen).

Statistical Analyses. Data are presented as mean ± SEM. Statistical significance was assessed using a two-sided Student *t* test. *P* values >0.05 were considered to be nonsignificant and statistically significant *P* values <0.05 were represented as *.

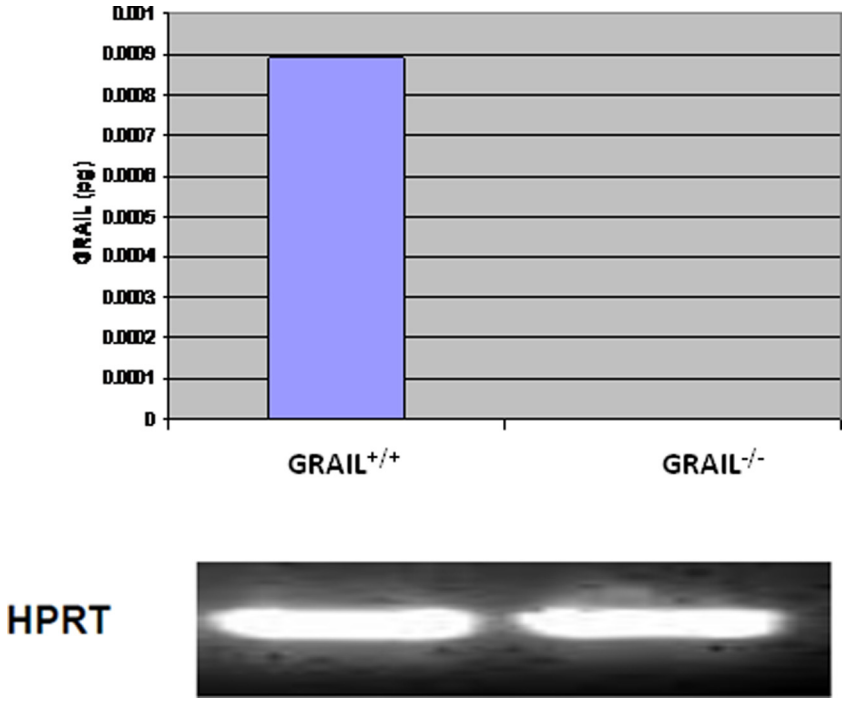

Fig. S1. Real-time PCR analysis of *Grail* RNA. Tissue from *Grail*$^{+/+}$ and *Grail*$^{-/-}$ mice was isolated, RNA was extracted and real-time PCR analysis was performed with a *Grail* specific probe as described in *Materials and Methods*. Absolute levels were quantified by spectrophotometry. Loss of *Grail* RNA is demonstrated by absence of quantifiable levels in KO sample despite amplification for 40 cycles. Equivalent amounts from each sample were also used for RT-PCR amplification of a constitutively expressed control gene (HPRT) confirming equal levels of RNA in both WT and KO.

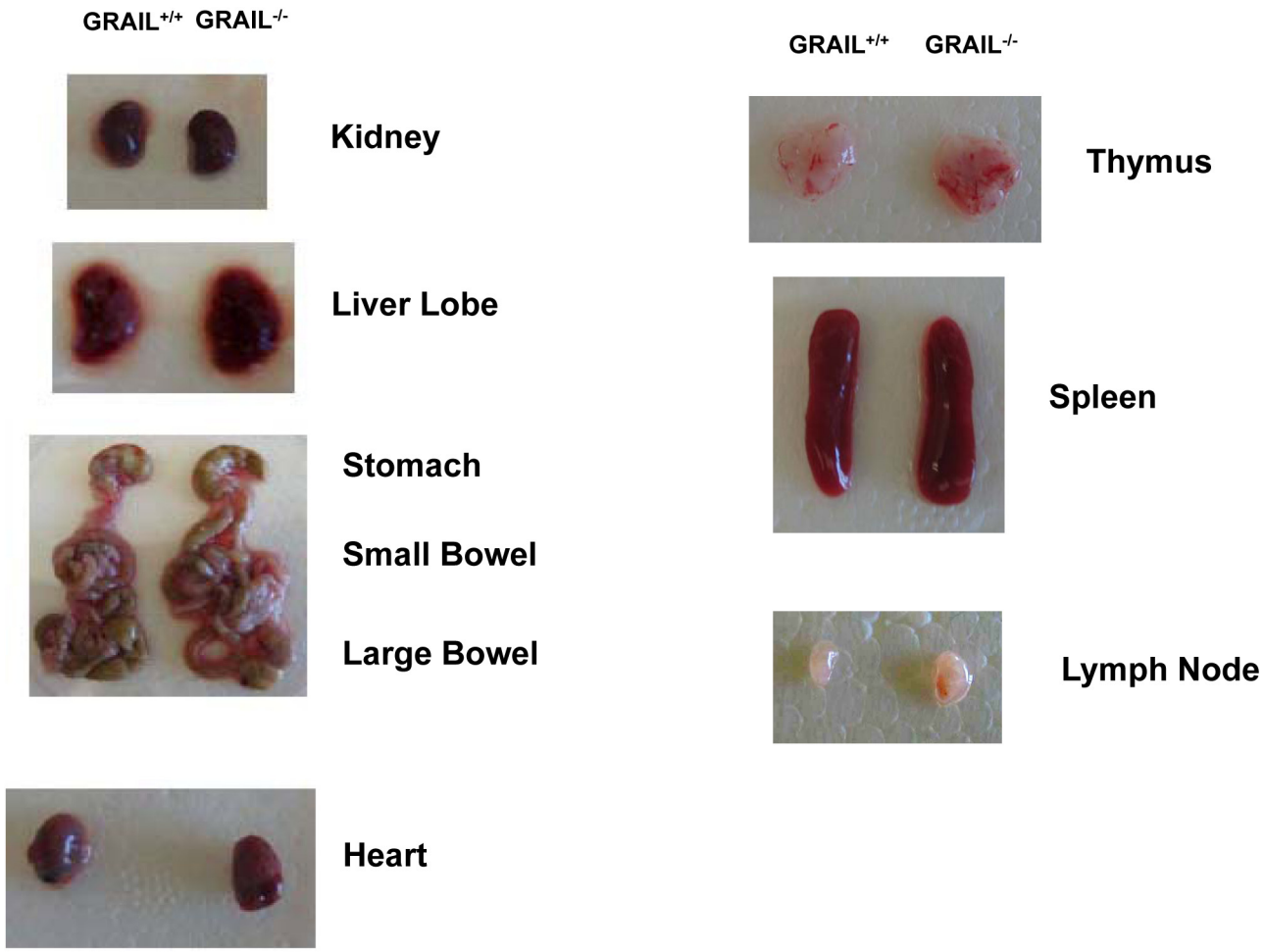

Fig. S2. Gross anatomy of organs from *Grail*$^{+/+}$ and *Grail*$^{-/-}$ mice. Comparison of the gross morphology of kidney, liver, intestine, heart, thymus, spleen and lymph node of 8-week-old *Grail*$^{+/+}$ and *Grail*$^{-/-}$ mice.

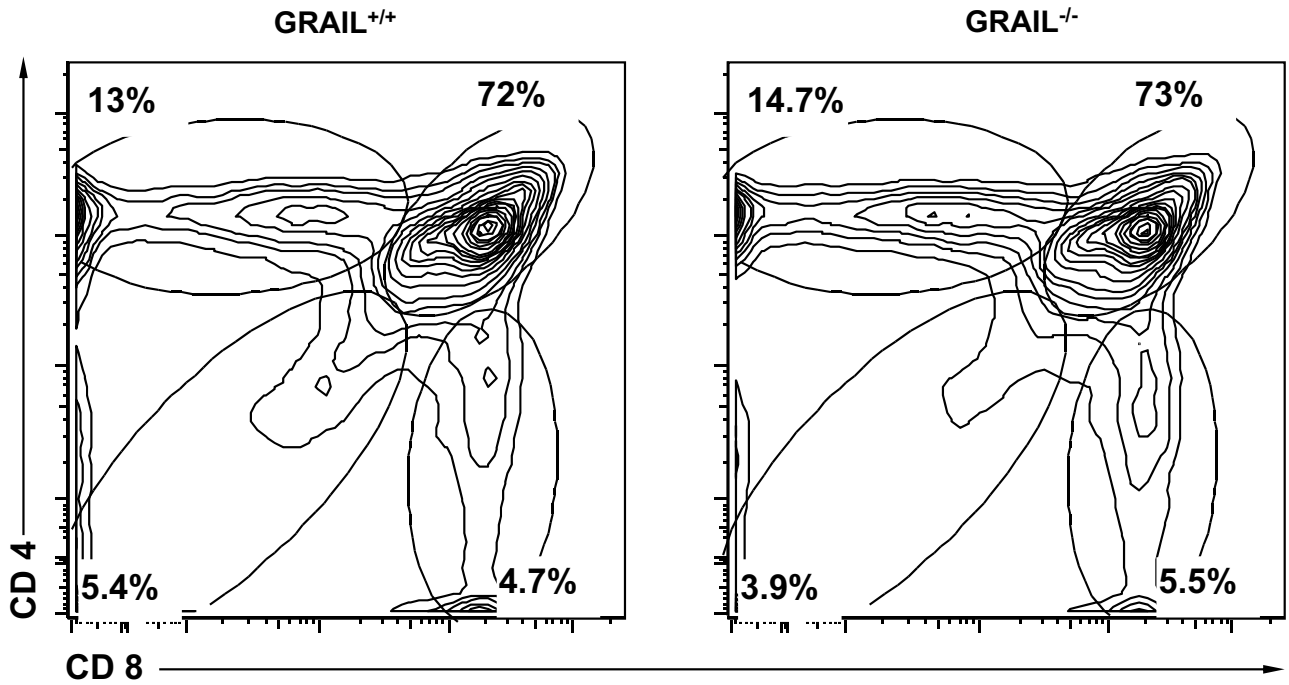

Fig. S3. Thymic development of T cells in *Grail*$^{+/+}$ and *Grail*$^{-/-}$ mice. Thymi from 8-week-old mice were homogenised and thymocytes were analyzed using flow cytometry. Four differentiation states of thymocytes were examined. Contour plots of double negative (CD4^{-} CD8^{-}), double positive (CD4^{+} CD8^{+}), and single positive (CD4^{-} CD8^{+}; CD4^{+} CD8^{-}) thymocytes are shown. No significant differences were found in the absence of *Grail*.

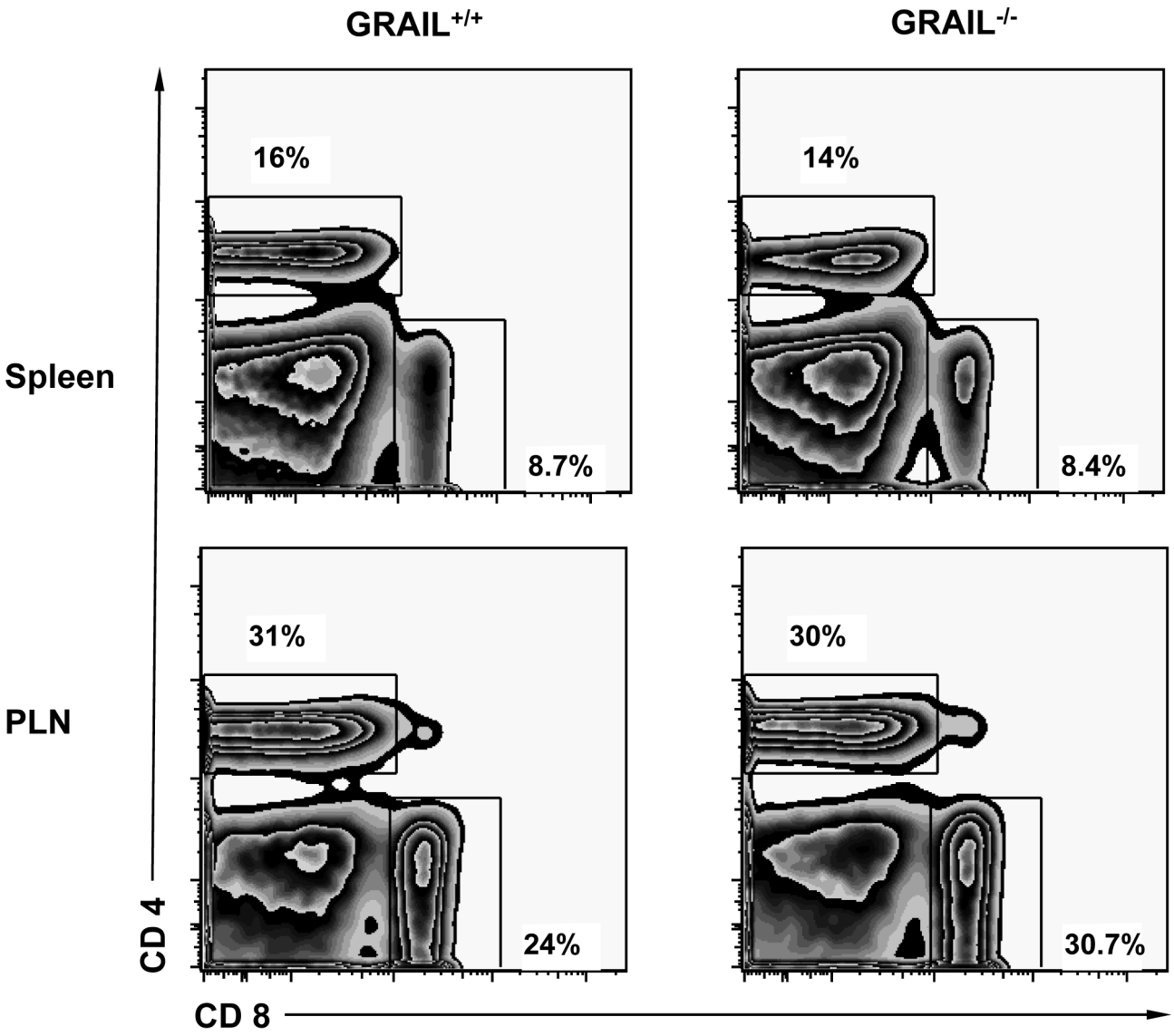

Fig. S4. Quantification of peripheral T cell subsets from *Grail*$^{+/+}$ and *Grail*$^{-/-}$ mice. CD4^{+} and CD8^{+} T cell subsets were analyzed using flow cytometry. Distributions of relative numbers from CD4^{+} and CD8^{+} T cell subsets are shown after isolation from spleens (*Upper*) or peripheral lymph nodes (PLN; *Lower*) from *Grail*$^{+/+}$ and *Grail*$^{-/-}$ mice. N.B.: Slight differences in CD8 T cell percentages were not significant across multiple samples.

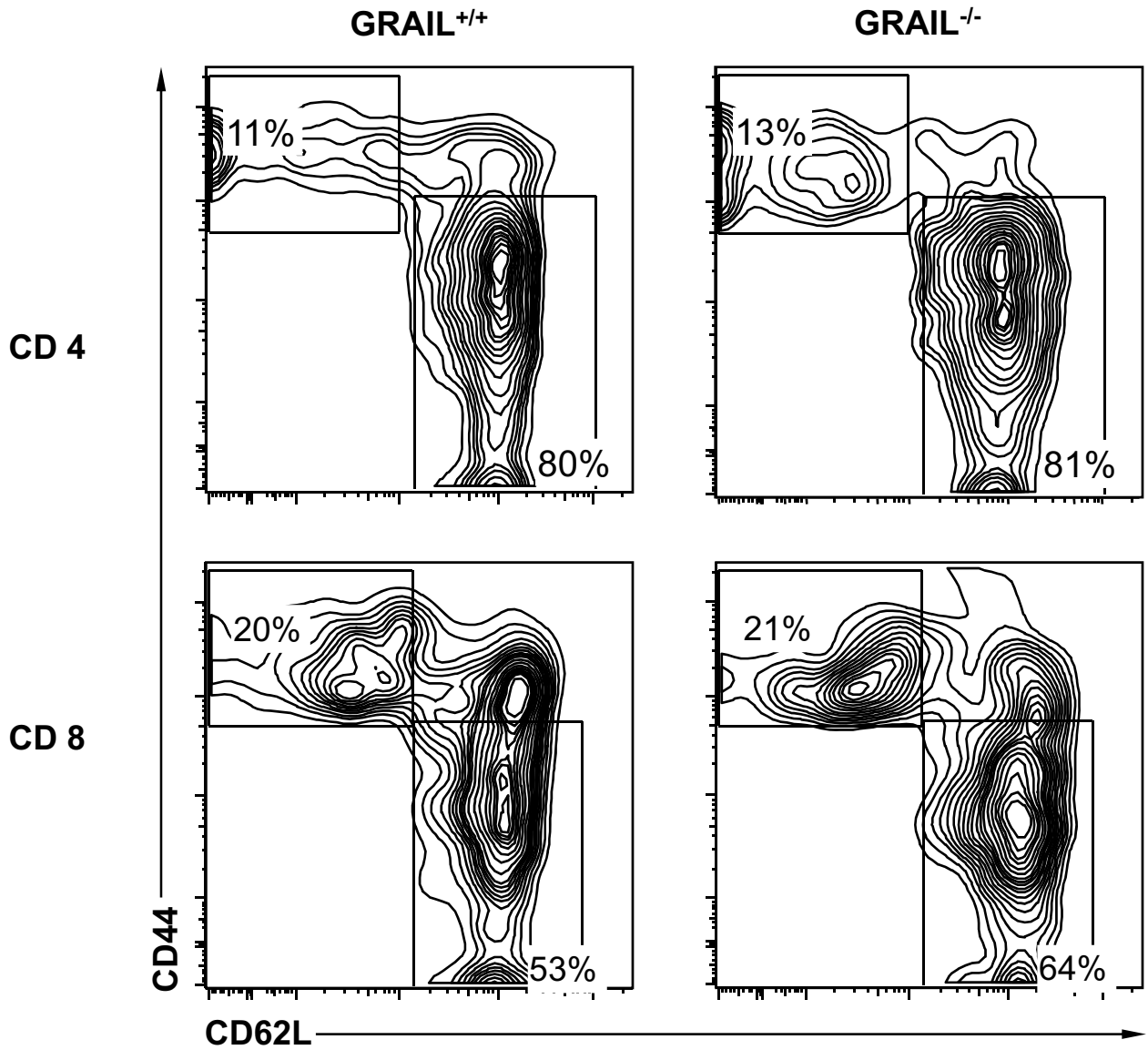

Fig. S5. Quantification of naïve and memory T cell subsets from *Grail*$^{+/+}$ and *Grail*$^{-/-}$ mice. Naïve and memory CD4^{+} and CD8^{+} T cell subpopulations were distinguished by flow cytometry using CD44 and CD62L markers after gating on CD4 (*Upper*) and CD8 (*Lower*). Distributions of relative numbers of naïve and memory CD4^{+} and CD8^{+} T cell subsets are shown from *Grail*$^{+/+}$ and *Grail*$^{-/-}$ mice at 8 weeks of age.

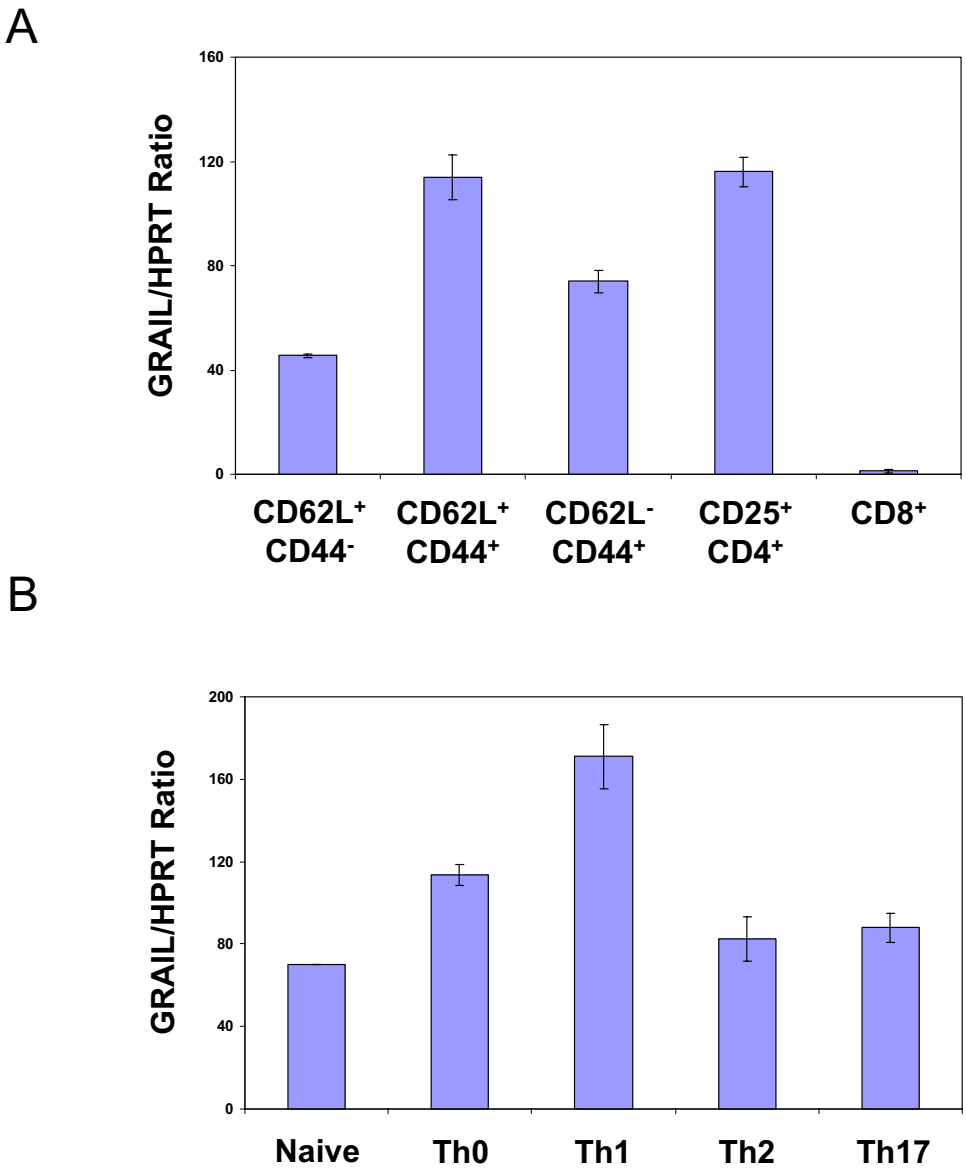

Fig. S6. Real-time PCR analysis of RNA from CD8+ and various $CD4^+$ T cell subsets. (*A* and *B*). Splenic $CD8^+$ T cells and $CD4^+$ T cell subpopulations (based on CD62L and CD44 staining) from *Grail*$^{+/+}$ and *Grail*$^{-/-}$ mice were isolated by cell sorting (*A*). For helper T cell subpopulations (*B*), sorted naïve $CD4^+$ T cells were first differentiated into Th0, Th1, Th2, and Th17 cells, respectively, for 3 days in culture as described in *Materials and Methods* before harvest and cell lysis. RNA was extracted from each T cell population and real-time PCR analysis was performed with a *Grail* specific probe as described in *Materials and Methods*. Shown are the mean values of duplicate samples. Input cDNA quantity was normalised according to HPRT (hypoxanthine guanine phosphoribosyl transferase) expression levels.

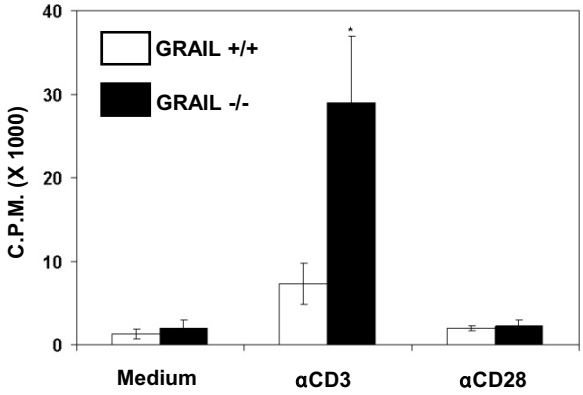

Fig. S7. Anti-CD3 versus anti-CD28 proliferation of naïve CD4$^+$ T cells from *Grail*$^{+/+}$ and *Grail*$^{-/-}$ mice. Splenic naïve CD4$^+$ T cells were stimulated with α-CD3 at 5 μg/mL or α-CD28 at 2 μg/mL for 48 h. Proliferation was measured by ^{3}H-thymidine incorporation.

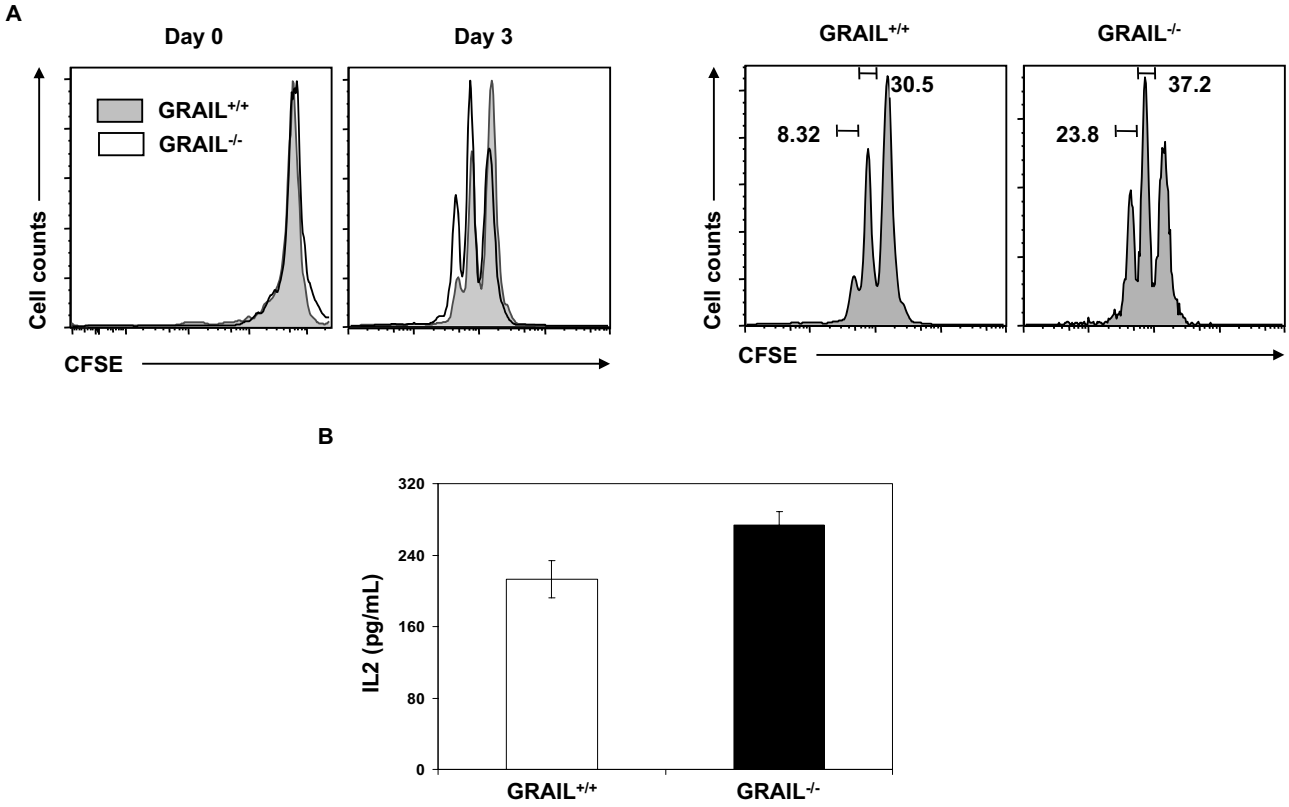

Fig. S8. Cycling and IL-2 secretion of naïve CD4$^+$ T cells from *Grail*$^{+/+}$ and *Grail*$^{-/-}$ mice after primary activation. (*A* and *B*) Naïve CD4$^+$ T cells were sorted from spleens of *Grail*$^{+/+}$ and *Grail*$^{-/-}$ mice, CFSE labeled and stimulated either with α-CD3 (5 μg/mL) and α-CD28 (2 μg/mL) (*A* and *B*). Proliferation was measured based on CFSE dilution after 72 h by flow cytometry (*A*). Histograms are shown comparing the proliferation between *Grail*$^{+/+}$ and *Grail*$^{-/-}$ T cells at day 0 and day 3 ((A), two panels on the *Left*). Percentage of cells proliferating in each cycling wave at day 3 is shown as well (*A*, *Right*). Supernatants were collected and IL-2 levels were measured by ELISA after 12 h of stimulation (*B*). Statistical analysis did not show significant differences between IL-2 secretion from WT and KO.

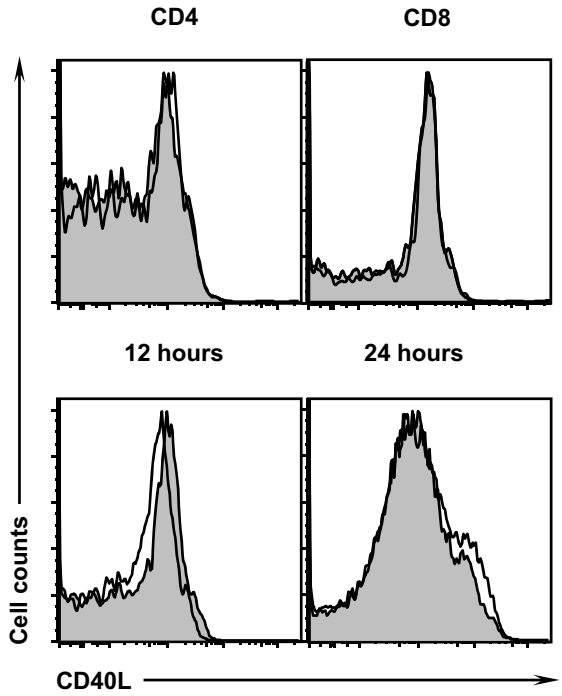

Fig. S9. Surface expression of CD40L on T cells. Baseline expression on $CD4^+$ and $CD8^+$ T cell subsets of $Grail^{+/+}$ (gray histograms) and $Grail^{-/-}$ (white histograms) mice measured by flow cytometry (*Upper*). Surface expression of CD40L in naïve $CD4^+$ T cells after 12 h of TCR stimulation measured by flow cytometry (*Lower*).

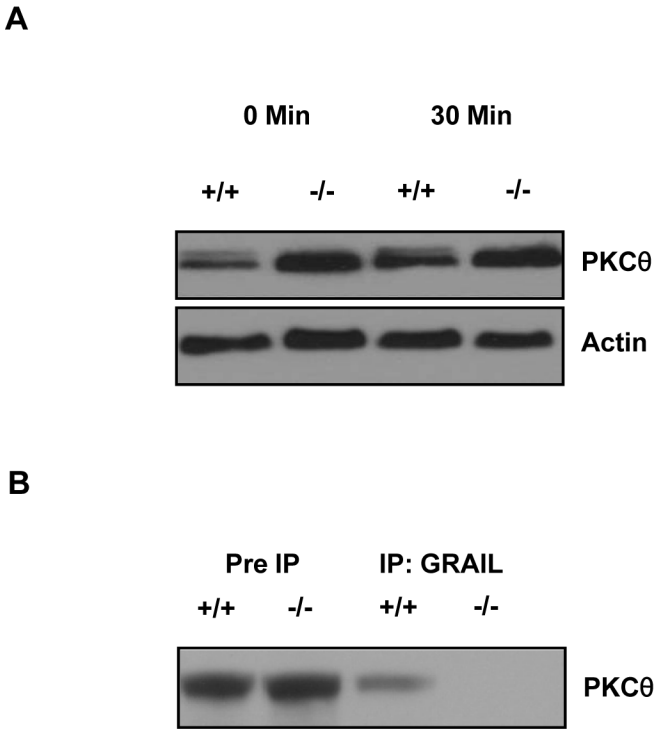

Fig. S10. *Grail* deficiency in T cells leads to increased levels of PKCθ. (*A*) Western blot analysis of PKCθ. Naïve CD4$^+$ T cells were sorted from spleens of *Grail*$^{+/+}$ and *Grail*$^{-/-}$ mice, and stimulated with α-CD3 (5 μg/mL) and α-CD28 (2 μg/mL) for 30 min. Cells were harvested, lysed and Western blot analysis was performed using antibodies against PKCθ. (*B*) CD4$^+$ T cells were sorted from spleens of *Grail*$^{+/+}$ and *Grail*$^{-/-}$ mice and stimulated with α-CD3 (5 μg/mL) and α-CD28 (2 μg/mL) for 60 min. Cell lysates were immunoprecipitated using GRAIL antibodies. Precipitates were subjected to immunoblotting and detected using PKCθ.